

반응 경로의 일의적 함수 (제 2 보). Thermal Electrocyclic Reaction에 대한 응용

金鎬濂[†] · 張孝元

서울대학교 자연과학대학 화학과

(1987. 12. 18 접수)

A Unique Function of Reaction Path(II). Applications to Thermal Electrocyclic Reactions

Hojing Kim[†] and Hyo Weon Jang

Department of Chemistry, College of Natural Sciences, Seoul National University, Seoul 151-742, Korea

(Received December 18, 1987)

요 약. thermal ring opening reaction의 가능한 두 반응 경로에 대한 근사적 반응 경로 함수, 그 함수의 norm 과 근사적 반응경로 평균 에너지를 계산, 비교하였다. 이 예들은, 큰 norm 과 적은 평균 에너지의 경로가 다른 경로에 비해 낮은 에너지 장벽을 갖는다는 가정을 명백히 증명했다.

ABSTRACT. For two possible paths of thermal ring opening reactions, the approximate reaction path functions, their norms and the approximate reaction path average energies are computed and compared. Illustrated examples clearly justify the postulate that the path with larger norm and lower average energy has lower barrier height than the other.

INTRODUCTION

The approximate forms of the reaction path function and the reaction path average energy are suggested in the preceding work.¹ These quantities are calculated for four thermal electrocyclic reactions, that is, thermal ring opening reactions of 1-chlorocyclobutene, 2-azetene, *cis*-2-chloro-3-fluorooxirane, 2-fluorocyclopropyl cation. To find the energy minimum path from a reactant to a product, reaction coordinate method is used.² That is, picking and fixing one or more variables from 3N-6 degrees of freedom as assumed reaction coordinate, SCF calculation is carried out while the other variables are optimized. MNDO method^{3,4} is used for SCF MO calculation. Since the resulting

semiempirical MO's neglect atomic orbital overlaps,⁵ they are renormalized in order to include overlaps between atomic orbitals. The relative magnitudes of two norms of the approximate reaction path functions and the approximate reaction path average energies consistently justify the allowedness of one specific path.

STEPS OF CALCULATION

Ground Electronic Wave Function. A single Slater determinant composed of doubly occupied semiempirical SCF MO's is used for a ground electronic wave function. In fact, all the reacting systems tested in the present work have closed shell electronic configurations in ground state. MNDO method^{3,4} is used to calculate MO's and potential energies. The MO's

Table 1. H₂O MO's

MO/AO	O1s	O2s	O2p _x	O2p _y	O2p _z	H1s	H2s
A ^a	0.996	0.015	0.000	0.000	0.003	-0.004	-0.004
B ^b	—	—	—	—	—	—	—
A	-0.222	0.843	0.000	0.132	0.000	0.152	0.152
B	—	0.873	0.000	0.138	0.000	0.123	0.123
A	0.000	0.000	0.624	0.000	0.000	0.424	-0.424
B	—	0.000	0.631	0.000	0.000	0.445	-0.445
A	0.093	-0.516	0.000	0.787	0.000	0.264	0.264
B	—	-0.482	0.000	0.765	0.000	0.313	0.313
A	0.000	0.000	0.000	0.000	1.000	0.000	0.000
B	—	0.000	0.000	0.000	1.000	0.000	0.000

^a ab initio minimal-basis-set MO. AO is single STO, with orbital exponents 1.27 for H1s, 7.66 for O1s, 2.25 for O2s, 2.21 for O2p, at experimental geometry⁹. ^b overlap normalized MNDO MO. AO is single STO, with orbital exponents 1.33 for H1s, 2.70 for O2s, 2.70 for O2p, at optimized geometry. (present calculation)³.

in semiempirical SCF MO method, including MNDO method, are made of valence atomic orbitals. The MO's are not overlap normalized.⁵ Semiempirical SCF MO method neglects overlaps between atomic orbitals. Therefore the MO's must be transformed to overlap normalized MO's (eigenvectors)⁶, in advance of the overlap computation between the wave functions corresponding to two different nuclear configurations.

In practice, the necessary transform is carried out by symmetric orthogonalization,⁷

$$C_{ki} = \sum_{j=1}^N X_{kj} C'_{ji} = \sum_{j=1}^N (US^{-1/2}U^T)_{kj} C'_{ji} \quad (1)$$

$$S = U^T S U \quad (2)$$

$$\psi_i = C_{1i}\alpha_1 + C_{2i}\alpha_2 + \dots$$

(overlap normalized MO)

$$\phi_i = C'_{1i}\alpha_1 + C'_{2i}\alpha_2 + \dots$$

$$\text{(MNDO MO), } (C'^T C')_{ij} = \delta_{ij}^5, \quad (3)$$

where α_i is basis orbital, S is overlap matrix of α_i 's is diagonalized form of S , and U is unitary matrix for S -to- s transformation. The orthonormal nature of ψ_i 's may be confirmed by:

$$\begin{aligned} \langle \psi_i | \psi_j \rangle &= \sum_{k,l=1}^N C_{ki} \langle \alpha_k | \alpha_l \rangle C_{lj} = (C^T S C)_{ij} \\ &= ((X C')^T S (X C'))_{ij} = (C'^T X^T S X C')_{ij} \\ &= (C'^T (U S^{-1/2} U^T)^T S (U S^{-1/2} U^T) C')_{ij} \end{aligned}$$

$$\begin{aligned} &= (C'^T U S^{-1/2} U^T S U S^{-1/2} U^T C')_{ij} \\ &= (C'^T U S^{-1/2} S S^{-1/2} U^T C')_{ij} \\ &= (C'^T U U^T C')_{ij} = (C'^T C')_{ij} = \delta_{ij}, \quad (4) \end{aligned}$$

where C and C' are matrices composed of elements, C_{ij} and C'_{ij} , respectively.

These overlap normalized MO's may be considered as good approximation to ab initio SCF MO's as being exemplified for H₂O in Table 1. Thus, in practice, a single Slater determinant made of solely valence MO's is used for a ground electronic wave function, $R(x)$, in the present calculation.

The overlap integral, $\langle R(x) | R(y) \rangle$, between the wave functions of two different nuclear configurations, which is needed to find the approximate reaction path function, F_N , is computed with the following steps:

1. Obtain semiempirical SCF MO's and potential energy at each point along a reaction path.
2. Transform semiempirical SCF MO's to overlap normalized MO's by symmetric orthogonalization.
3. Transform each nuclear configuration to principal axis frame, also for its MO's. And

- construct single Slater determinant from occupied overlap normalized MO's.
- Superimpose two principal axis frames corresponding to each nuclear configuration so that the continuity of $g_1(x)$ is guaranteed. (to satisfy the definition of $g_1(x)$)
 - Calculate $\langle R(x)|R(y)\rangle$ in this relative locations, using single Slater determinants. STO's with MNDO exponents³ are used as atomic orbitals (Fig. 1).

Potential Energy Minimum Path-Reaction

Path. It is generally assumed that most of the reactant molecules, in the Born-Oppenheimer approximation, follow the energy minimum path among many possible paths which connect the reactant point to the product point on a potential energy surface. So, to find the reaction path function, one should determine which is the energy minimum path representing the actual reaction path. A reaction path implies an energy minimum path in this study.

In reaction coordinate method, used in this work, one or more variables which contribute reaction coordinate mostly are chosen among $3N-6$ degrees of freedom. And these variables are changed monotonously from reactant values to product ones, while all other variables are optimized.²

Initially one variable is chosen to determine the reaction path. If the variable gives different paths for forward and reverse direction, one more variable is added. Then the two variables are changed systematically in the region where "chemical hysteresis"⁹ is shown. And the tran-

sition state is the point of the highest potential energy on the energy minimum path. Although the reaction coordinate of the reaction is composed mostly of the chosen variables, the calculated energy minimum path does not exactly coincide with the reaction coordinate.

CALCULATION AND DISCUSSION

In this work, four reacting systems are chosen. They are thermal ring opening reactions of 2-chlorocyclobutene, 2-azetene, *cis*-2-chloro-3-fluorooxirane and 2-fluorocyclopropyl cation. They are all classified as thermal electrocyclic reactions.

They represent

4 π electron-homogeneous 4 membered ring system,

4 π electron-heterogeneous 4 membered ring system,

4 π electron-heterogeneous 3 membered ring system,

2 π electron-homogeneous 3 membered ring system, respectively.

Their products of ring opening reactions are expected to be two stereoisomers. Naive application of Woodward-Hoffmann rule does not tell which one is preferred. Theoretical attempts have been made to confirm the preferred product. Generally It is assumed that larger substituent rotates outward, apart from the skeleton of the product molecule, during the Woodward-Hoffmann-rule-predicted-rotation, because of steric hindrance.¹⁰ In some cases, however, it is not true.¹¹

A generalization has been made by Rondan and Houk. They consider more than steric factor.¹² The reaction path function also provides a criterion on the rotational directions of the terminal substituents in ring opening reaction.

In the following four examples, the two reaction paths, from ring form to two opened



Fig. 1. Two nuclear configurations in principal axis frame and their relative locations to calculate $\langle R(x)|R(y)\rangle$ (straight lines are principal axes).

forms, are considered. The ground electronic wave functions and the potential energies are obtained at some intervals along each energy minimum path determined by reaction coordinate method mentioned above. And the transition states are located by potential energies. The potential energy barrier height is computed for each path. The barrier height is used as a criterion of the allowedness of a specific path against another one. On the other hand, the approximate reaction path function, the norm of the approximate reaction path function and the approximate reaction path average energy are calculated for each path and the norms and the average energies are compared. A successive refinement of approximation is made by increasing nuclear configurations included in the function. If the approximate reaction path function is constructed from N wave functions, then the lower bound of the norm is $N^{-1/2}$.

Ring Opening Reaction of 3-chlorocyclobutene. The unsubstituted molecule of the reactant, cyclobutene, gives ring opened product, butadiene, through symmetry allowed conrotatory

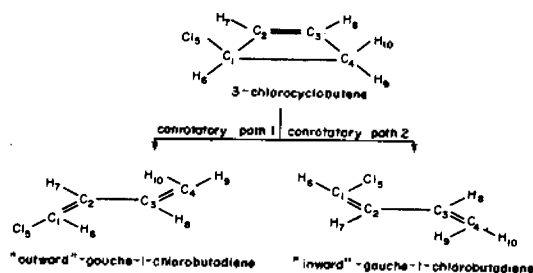


Fig. 2. Scheme of the reaction.

path.¹³ In the past it is assumed that the product butadiene is *cis* form, but it is now accepted that the *cis*-butadiene is not a stable form. The stable nuclear configurations of butadiene are *gauche*-butadiene and *trans*-butadiene, according to semiempirical¹² and ab initio calculation.¹⁴

Present calculation also indicates that the ring opened product of 3-chlorocyclobutene is not *cis*-1-chlorobutadiene but *gauche*-1-chlorobutadiene (Fig. 2). The allowed product of this reaction is "outward"-*gauche*-1-chlorobutadiene. This is confirmed by present calculation and experiment¹⁵ (Table 2). Some selected nuclear configurations and their relative locations in principal axis frame are illustrated for each path in Fig. 3.

Table 2. Energies and fixed variable values along each path

point number	Path 1			Path 2		
	$R(\text{\AA})^a$	$D(\text{deg})^b$	potential energy ^c	$D(\text{deg})^b$	$R(\text{\AA})^a$	
1	3.20	181.2	18.69154	19.31887	3.33	
2	3.00	180.0	19.71985	23.25168	3.00	
3	2.70	175.9	28.01413	35.64721	2.70	
4	2.40	169.5	46.39295	56.90289	2.40	
5	2.13	141.2 ^d	68.04574 ^e	75.61482 ^e	2.18	
6	1.80	114.7	34.69481	34.89467	1.80	
7	1.57	118.3	22.32285	22.32285	1.57	
energy barrier	$\Delta E_{\text{forward}} = 45.72289$ $\Delta E_{\text{reverse}} = 49.35420$			$\Delta E_{\text{forward}} = 53.29197$ $\Delta E_{\text{reverse}} = 56.29595$		
	allowed path			forbidden path		

^a bond length of C₁-C₄. ^b dihedral angle of Cl₅-C₁-C₂-C₃. ^c energy unit is kcal/mole. ^d except these points all other D's are optimized. ^e transition state. note: point number 1,7 correspond to ring opened product molecules and ring form reactant molecule respectively.

Table 3. The approximate reaction path functions for each path, $F_N = \sum_{i=1}^N R(x_i) \Delta_i \equiv \sum_{i=1}^N \psi_i \Delta_i$

N	F_N of Path 1	F_N of Path 2
3	$0.33566\psi_1 + 0.33217\psi_5 + 0.33217\psi_7$	$0.33335\psi_1 + 0.33331\psi_4 + 0.33335\psi_7$
4	$0.25376\psi_1 + 0.24603\psi_4 + 0.24625\psi_5 + 0.25396\psi_7$	$0.25394\psi_1 + 0.24556\psi_3 + 0.24608\psi_5 + 0.25443\psi_7$
5	$0.17606\psi_1 + 0.17303\psi_2 + 0.21239\psi_4 + 0.21593\psi_5 + 0.22258\psi_7$	$0.20153\psi_1 + 0.19798\psi_2 + 0.18901\psi_4 + 0.19147\psi_5 + 0.22001\psi_7$
6	$0.16668\psi_1 + 0.16381\psi_2 + 0.20113\psi_4 + 0.20272\psi_5 + 0.13076\psi_6 + 0.13490\psi_7$	$0.19580\psi_1 + 0.15662\psi_2 + 0.10554\psi_3 + 0.14596\psi_4 + 0.18523\psi_5 + 0.21086\psi_7$
7	$0.15777\psi_1 + 0.13644\psi_2 + 0.079561\psi_3 + 0.16796\psi_4 + 0.19881\psi_5 + 0.12769\psi_6 + 0.13176\psi_7$	$0.19091\psi_1 + 0.15272\psi_2 + 0.10289\psi_3 + 0.14245\psi_4 + 0.17963\psi_5 + 0.11257\psi_6 + 0.11884\psi_7$

^a ψ_i refers to wave function at the point number i .

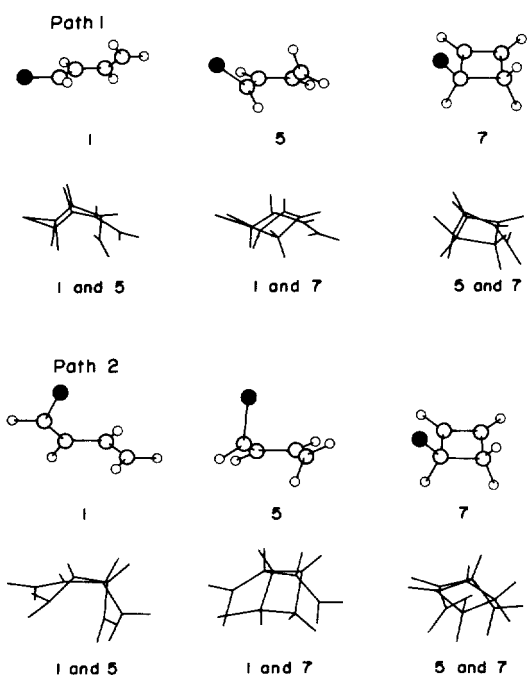


Fig. 3. Selected nuclear configurations and their relative locations in principal axis frame along each path.

The results of the present method are listed in Table 3~5.

Ring Opening Reaction of 2-azetine. Because of the electron lone pair of nitrogen, the

Table 4. The norms of the approximate reaction path functions for each path and their ratio

N	$\ F_N\ $ of Path 1	$\ F_N\ _{P1}/\ F_N\ _{P2}$ ^a	$\ F_N\ $ of Path 2
3	0.57937	1.0034	0.57739
4	0.50651	1.0026	0.50522
5	0.47419	1.0095	0.46975
6	0.46139	1.0033	0.45988
7	0.45598	1.0041	0.45411

^a P1 means path 1, P2 means path 2.

Table 5. The approximate reaction path average energies, $E_{RP}(N)$ ^a, for each path

N	Path 1	Path 2	$E_{RP}(N)$ (Path2) - $E_{RP}(N)$ (Path1)
3	36.292	32.847	-3.445
4	38.583	37.946	-0.637
5	36.218	38.641	2.423
6	37.019	38.205	1.186
7	36.560	39.176	2.616

^a Energy unit is kcal/mole.

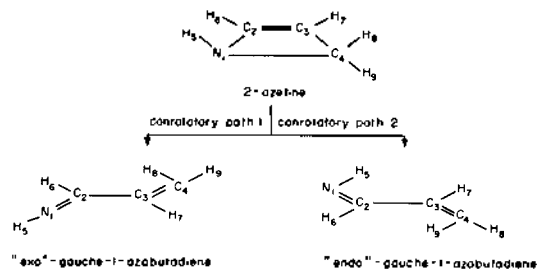


Fig. 4. Scheme of the reaction.

Table 6. Energies and fixed variable values along each path

point number	Path 1			Path 2		
	$R(\text{\AA})^a$	$D(\text{deg})^b$	potential energy ^c	$D(\text{deg})^b$	$R(\text{\AA})^a$	
1	3.01	180.4	32.91645	33.48389	-0.2	3.17
2	2.80	180.1	34.49021	40.56195	3.9	2.80
3	2.40	179.7	50.18428	67.59318	17.4	2.40
4	2.20	176.9	66.25531	88.57543	28.6	2.20
5	1.98	157.0	82.88981 ^e	103.2467 ^e	59.4 ^d	2.06
6	1.80	116.8	66.61800	67.35961	105.0 ^d	1.80
7	1.51	120.1	45.38429	45.38429	120.1	1.51
energy barrier	$\Delta E_{\text{forward}}=37.50552$ $\Delta E_{\text{reverse}}=49.97336$			$\Delta E_{\text{forward}}=57.86242$ $\Delta E_{\text{reverse}}=69.76282$		
	allowed path			forbidden path		

^a bond length of $\text{N}_1\text{-C}_4$. ^b dihedral angle of $\text{H}_5\text{-N}_1\text{-C}_2\text{-C}_3$. ^c energy unit is kcal/mol. ^d except these points all other D 's are optimized. ^e transition state. note: point number 1,7 correspond to ring opened product molecules and ring form reactant molecule respectively.

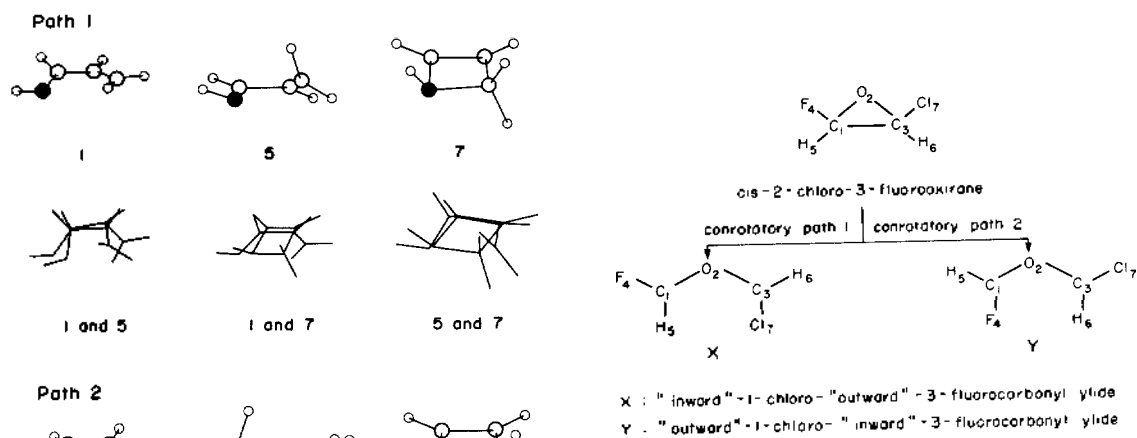


Fig. 6. Scheme of the reaction.

Fig. 5. Selected nuclear configurations and their relative locations in principal axis frame along each path.

product of this reaction, 1-azabutadiene, exists as two stereoisomers of *endo* and *exo*, depending

on $\text{N}_1\text{-H}_5$ orientations in the ring opened product (Fig. 4). As in the case of above example, the ring opened product, 1-azabutadiene, is not a planar form but a *gauche* form. The allowed product of this reaction is predicted to be "*exo*"-*gauche*-1-azabutadiene by present calculation (Table 6). Some selected nuclear configurations and their relative locations in principal axis frame are illustrated for each path in Fig. 5.

The results of the present method are listed in Table 7~9.

Table 7. The approximate reaction path functions for each path, $F_N = \sum_{i=1}^N R(x_i) \Delta_i \equiv \sum_{i=1}^N \psi_i \Delta_i$

N	F_N of path 1	F_N of path 2
3	$0.34608\psi_1 + 0.32628\psi_5 + 0.32764\psi_7$	$0.33345\psi_1 + 0.33145\psi_4 + 0.33511\psi_7$
4	$0.24397\psi_1 + 0.22960\psi_3 + 0.25667\psi_5 + 0.26976\psi_7$	$0.28015\psi_1 + 0.27552\psi_4 + 0.22050\psi_6 + 0.22382\psi_7$
5	$0.22218\psi_1 + 0.21084\psi_3 + 0.19896\psi_5 + 0.16106\psi_6 + 0.20696\psi_7$	$0.24441\psi_1 + 0.20344\psi_3 + 0.17549\psi_5 + 0.17538\psi_6 + 0.20128\psi_7$
6	$0.21906\psi_1 + 0.15483\psi_3 + 0.099609\psi_4 + 0.16231\psi_5 + 0.16222\psi_6 + 0.20198\psi_7$	$0.20236\psi_1 + 0.081224\psi_2 + 0.16858\psi_3 + 0.17796\psi_5 + 0.17187\psi_6 + 0.19801\psi_7$
7	$0.19533\psi_1 + 0.039825\psi_2 + 0.13510\psi_3 + 0.10576\psi_4 + 0.16051\psi_5 + 0.16202\psi_6 + 0.20146\psi_7$	$0.19478\psi_1 + 0.098313\psi_2 + 0.10639\psi_3 + 0.078172\psi_4 + 0.15219\psi_5 + 0.17350\psi_6 + 0.19665\psi_7$

ψ_i refers to wave function at the point number i .

Table 8. The norms of the approximate reaction path functions for each path and their ratio

N	$\ F_N\ $ of path 1	$\ F_N\ _{P1}/\ F_N\ _{P2}$ ^a	$\ F_N\ $ of path 2
3	0.58931	1.0151	0.58057
4	0.53408	1.0037	0.53213
5	0.50986	1.0083	0.50566
6	0.50352	1.0039	0.50156
7	0.50290	1.0062	0.49979

^a P1 means Path 1, P2 means Path 2.

Table 9. The approximate reaction path average energies, $E_{RP}(N)$ ^a, for each path

N	Path 1	Path 2	$E_{RP}(N)$ (Path 2) - $E_{RP}(N)$ (Path 1)
3	53.307	55.732	2.425
4	53.071	58.796	5.725
5	54.508	61.002	6.494
6	55.007	60.402	5.395
7	54.831	60.950	6.119

^a energy unit is kcal/mole.

Table 10. Energies and fixed variable values along each path

point number	Path 1			Path 2		
	$A(\text{deg})$ ^a	$D(\text{deg})$ ^b	Potential energy ^c	$D(\text{deg})$ ^b	$A(\text{deg})$ ^a	
1	128.4	180.0	-44.83901	-44.48386	0.0	129.7
2	115.0	180.0	-40.11017	-38.42518	0.0	115.0
3	105.0	165.3	-28.92256	-25.62452	35.4	105.0
4	100.1	136.0	-24.97584 ^d	-22.30776 ^d	68.0	101.2
5	80.0	108.7	-55.46471	-55.46471	108.7	80.0
6	70.0	112.4	-68.60270	-68.60270	112.4	70.0
7	65.7	113.9	-70.36866	-70.36866	113.9	65.7
energy barrier	$\Delta E_{\text{forward}} = 45.39282$ $\Delta E_{\text{reverse}} = 19.86317$			$\Delta E_{\text{forward}} = 48.06090$ $\Delta E_{\text{reverse}} = 22.17610$		
	allowed path			forbidden path		

^a Bond angle of $C_1-O_2-C_3$. ^b dihedral angle of $F_4-C_1-O_2-C_3$. ^c energy unit is kcal/mol. ^d transition state. Note: point number 1,7 correspond to ring opened product molecules and ring form reactant molecule respectively. All D's are optimized.

Ring Opening Reaction of *cis*-2-chloro-3-fluoroepoxide. The ring opened products of this reaction are all planar (Fig. 6). The allowed product of this reaction is predicted to be "inward" -1-chloro- "outward" -3-fluorocarbonyl ylide by present calculation (Table 10). Some selected nuclear configurations and their relative locations in principal axis frame are illustrated for each path in Fig. 7.

The results of the present method are listed in Table 11~13.

Ring Opening Reaction of 2-fluorocyclopropyl Cation. The ring opened products of this reaction are all planar (Fig. 8). The allowed product of this reaction is predicted to be "outward"-1-fluoroallyl cation by present calculation (Table 14). Some selected nuclear configurations and their relative locations in principal axis frame are illustrated for each path in Fig. 9.

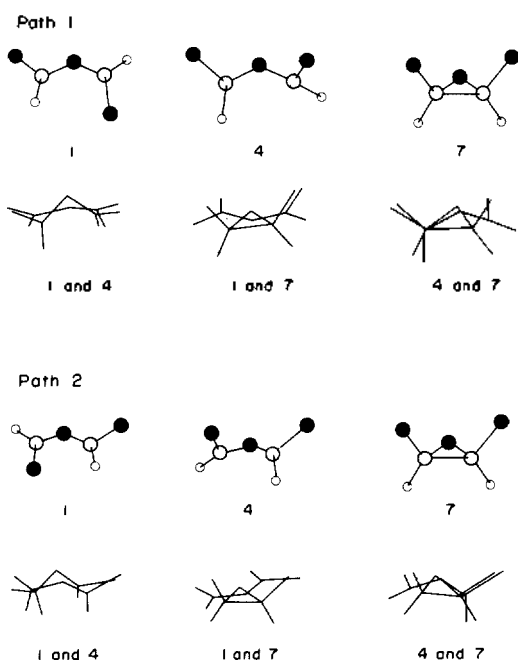


Fig. 7. Selected nuclear configurations and their relative locations in principal axis frame along each path.

Table 11. The approximate reaction path functions for each path, $F_N = \sum_{i=1}^N R(x_i) A_i \equiv \sum_{i=1}^N \psi_i A_i$

N	F_N of Path 1	F_N of Path 2
3	$0.33336\psi_1 + 0.33332\psi_4 + 0.33332\psi_7$	$0.33355\psi_1 + 0.33323\psi_4 + 0.33323\psi_7$
4	$0.24999\psi_1 + 0.24882\psi_3 + 0.25002\psi_4 + 0.25118\psi_7$	$0.25013\psi_1 + 0.24983\psi_3 + 0.24987\psi_4 + 0.25017\psi_7$
5	$0.17252\psi_1 + 0.15246\psi_2 + 0.21764\psi_3 + 0.22818\psi_4 + 0.22920\psi_7$	$0.18049\psi_1 + 0.17284\psi_2 + 0.21208\psi_3 + 0.21717\psi_4 + 0.21742\psi_7$
6	$0.16069\psi_1 + 0.14200\psi_2 + 0.20271\psi_3 + 0.21239\psi_4 + 0.14092\psi_5 + 0.14129\psi_7$	$0.16890\psi_1 + 0.16174\psi_2 + 0.19846\psi_3 + 0.20249\psi_4 + 0.13316\psi_5 + 0.13526\psi_7$

^a ψ_i refers to wave function at the point number i .

Table 12. The norms of the approximate reaction path functions for each path and their ratio

N	$\ F_N\ $ of Path 1	$\ F_N\ _{P1}/\ F_N\ _{P2}$	$\ F_N\ $ of Path 2
3	0.57737	0.99971	0.57754
4	0.50120	1.0016	0.50041
5	0.47877	1.0263	0.46651
6	0.46206	1.0239	0.45128

^a P1 means Path 1, P2 means Path 2.

Table 13. The approximate reaction path average energies, $E_{RP}(N)$ ^a, for each path

N	Path 1	Path 2	$E_{RP}(N)$ (Path2) - $E_{RP}(N)$ (Path1)
3	-46.728	-45.720	1.008
4	-42.325	-40.707	1.618
5	-41.973	-40.249	1.724
6	-41.827	-40.234	1.593

^a energy unit is kcal/mole.

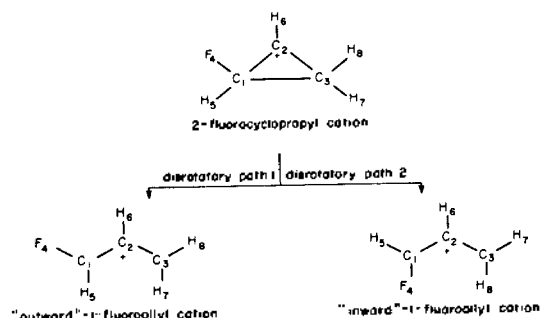


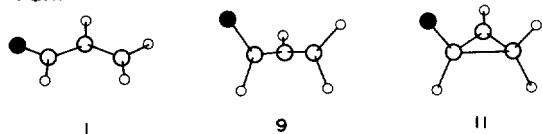
Fig. 8. Scheme of the reaction.

Table 14. Energies and fixed variable values along each path

point number	Path 1			Path 2		
	A(deg) ^a	D(deg) ^b	potential energy ^c	D(deg) ^b	A(deg) ^a	
1	124.7	180.0	172.0859	171.5015	0.0	128.9
2	110.0	178.9	177.4793	181.6924	1.4	110.0
3	100.0	180.0	188.5757	197.0478	34.3	100.0
4	95.0	160.3	196.9853	205.5963	55.0	95.0
5	90.0	140.2	205.7280	213.9012	65.3	90.0
6	85.0	129.9	213.5447	221.4777	73.1	85.0
7	81.0	123.8	218.7328	226.4364	78.3	81.0
8	72.4	117.8	225.3468	231.5748 ^e	92.5	72.4
9	68.4	115.1	226.0365 ^e	229.3252	100.0 ^d	68.4
10	66.0	113.7	225.8220	226.2900	108.0 ^d	66.0
11	63.0	112.2	225.4650	225.4650	112.2	63.0
energy barrier	$\Delta E_{\text{forward}}=0.5715$ $\Delta E_{\text{reverse}}=53.9506$			$\Delta E_{\text{forward}}=6.1098$ $\Delta E_{\text{reverse}}=60.0732$		
	allowed path			forbidden path		

^a angle of C₁-O₂-C₃. ^b dihedral angle of F₄-C₁-C₂-C₃. ^c energy unit is kcal/mole. ^d except these points all other D's are optimized. ^e transition state. note: point number 1, 11 correspond to ring opened product molecules and ring form reactant molecule respectively.

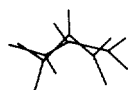
Path 1



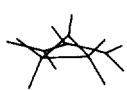
1

9

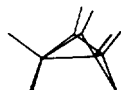
11



1 and 9

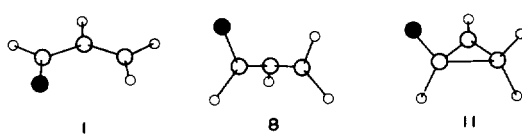


1 and 11



9 and 11

Path 2



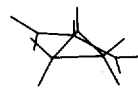
1

8

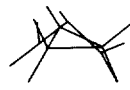
11



1 and 8



1 and 11



8 and 11

Table 15. The approximate reaction path functions for each path, $F_N = \sum_{i=1}^N R(x_i) \Delta_i \equiv \sum_{i=1}^N \psi_i \Delta_i$

N	F_N of path 1	F_N of path 2
3	$0.33294\psi_1 + 0.33163\psi_5 + 0.33543\psi_{11}$	$0.33331\psi_1 + 0.33177\psi_5 + 0.33492\psi_{11}$
4	$0.25104\psi_1 + 0.24005\psi_4 + 0.24936\psi_7 + 0.25955\psi_{11}$	$0.25364\psi_1 + 0.22645\psi_3 + 0.24838\psi_7 + 0.27154\psi_{11}$
5	$0.20413\psi_1 + 0.18540\psi_3 + 0.18261\psi_5 + 0.18190\psi_7 + 0.24596\psi_{11}$	$0.18462\psi_1 + 0.14978\psi_2 + 0.22506\psi_4 + 0.21167\psi_8 + 0.22887\psi_{11}$
6	$0.19981\psi_1 + 0.18043\psi_3 + 0.19140\psi_5 + 0.12342\psi_7 + 0.09822\psi_8 + 0.20672\psi_{11}$	$0.18777\psi_1 + 0.11010\psi_2 + 0.12331\psi_3 + 0.16571\psi_5 + 0.18862\psi_8 + 0.22449\psi_{11}$
7	$0.20077\psi_1 + 0.13811\psi_3 + 0.07729\psi_4 + 0.15308\psi_5 + 0.13330\psi_7 + 0.09205\psi_8 + 0.20539\psi_{11}$	$0.18482\psi_1 + 0.10864\psi_2 + 0.12070\psi_3 + 0.16516\psi_5 + 0.17169\psi_8 + 0.09110\psi_9 + 0.15789\psi_{11}$
8	same above ^b	same above ^b
9	same above ^b	$0.17196\psi_1 + 0.13604\psi_2 + 0.06072\psi_3 + 0.14039\psi_4 + 0.013378\psi_5 + 0.098828\psi_7 + 0.12681\psi_8 + 0.096921\psi_9 + 0.15495\psi_{11}$

Fig. 9. Selected nuclear configurations and their relative locations in principal axis frame along each path.

^a ψ_i refers to wave function at the point number i .
^b see Ref. 1.

Table 16. The norms of the approximate reaction path functions for each path and their ratio

N	$\ F_N\ $ of Path 1	$\ F_N\ _{P1}/\ F_N\ _{P2}$	$\ F_N\ $ of Path 2
3	0.58027	1.0004	0.58003
4	0.52732	1.0001	0.52729
5	0.51005	0.99746	0.51135
6	0.50445	1.0008	0.50404
7	0.50137	1.0025	0.50014
8	0.50137	1.0025	0.50014
9	0.50137	1.0097	0.49656

* P1 means Path 1, P2 means Path 2.

Table 17. The approximate reaction path average energies, $E_{RP}(N)$ ^a, for each path

N	Path 1	Path 2	$E_{RP}(N)$ (Path2) - E_{RP} (N) (Path1)
3	201.15	203.64	2.49
4	203.55	205.58	2.03
5	202.90	205.77	2.87
6	203.52	206.24	2.72
7	203.52	206.80	3.28
8	203.52	206.80	3.28
9	203.52	206.81	3.29

^a energy unit is kcal/mole.

The results of the present methods are listed in Table 15~17.

CONCLUSION

Four examples illustrated justify that the norm of the reaction path function and the reaction path average energy can be used for the judgment of the allowedness of a specific reaction path against other possible ones. The path with lower barrier height has larger norm of the

function and lower average energy.

REFERENCES

1. H. Kim and H. W. Jang, *J. Korean Chem. Soc.*, **32**, 94 (1988).
2. J. W. McIver, Jr., and A. Komornicki, *J. Am. Chem. Soc.*, **94**, 2625 (1972).
3. M. J. S. Dewar and W. Thiel, *ibid.*, **99**, 4899, 4907 (1977).
4. J. Mckelvey, "A Modification of QCPE Program No. 353".
5. J. A. Pople and D. L. Beveridge, "Approximate Molecular Orbital Theory", P. 59ff, McGraw-Hill, New York, 1970.
6. D. R. Kelsey, *J. Comput. Chem.*, **1**, 3, 21 (1980).
7. A. Szabo and N. S. Ostlund, "Modern Quantum Chemistry", P. 173ff, Macmillan, New York, 1982.
8. I. N. Levine, "Quantum Chemistry", 3rd Ed., P. 427, Allyn and Bacon, 1983.
9. M. J. S. Dewar and S. Kirschner, *J. Am. Chem. Soc.*, **93**, 4292 (1971).
10. E. N. Marvell, "Thermal Electrocyclic Reactions", pp. 127ff, Academic Press, New York, 1980.
11. W. R. Dolbier, Jr., and H. Koroniak, *J. Am. Chem. Soc.*, **106**, 1871 (1984).
12. N. G. Rondan and K. N. Houk, *ibid.*, **107**, 2099 (1985).
13. J. Breulet and H. F. Schaefer III, *ibid.*, **106**, 1221 (1984).
14. C. W. Bock and M. Trachtman, *Chem. Phys.*, **93**, 431 (1985).
15. W. Kirmse, N. G. Rondan and K. N. Houk, *J. Am. Chem. Soc.*, **106**, 7989 (1984).